

Journal Pre-proof

Causal topography of visual cortex in perceptual learning

Paolo Capotosto, Giorgia Committeri, Antonello Baldassarre

PII: S1053-8119(19)30848-1

DOI: <https://doi.org/10.1016/j.neuroimage.2019.116257>

Reference: YNIMG 116257

To appear in: *NeuroImage*

Received Date: 24 July 2019

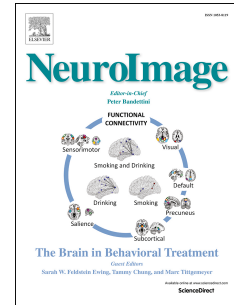
Revised Date: 26 September 2019

Accepted Date: 7 October 2019

Please cite this article as: Capotosto, P., Committeri, G., Baldassarre, A., Causal topography of visual cortex in perceptual learning, *NeuroImage* (2019), doi: <https://doi.org/10.1016/j.neuroimage.2019.116257>.

This is a PDF file of an article that has undergone enhancements after acceptance, such as the addition of a cover page and metadata, and formatting for readability, but it is not yet the definitive version of record. This version will undergo additional copyediting, typesetting and review before it is published in its final form, but we are providing this version to give early visibility of the article. Please note that, during the production process, errors may be discovered which could affect the content, and all legal disclaimers that apply to the journal pertain.

© 2019 Published by Elsevier Inc.



Causal topography of visual cortex in perceptual learning

Paolo Capotosto¹, Giorgia Committeri¹, Antonello Baldassarre¹

1. Department of Neuroscience, Imaging and Clinical Sciences, and ITAB, Institute of Advanced Biomedical Technologies University "G. D'Annunzio", Chieti, Italy

Corresponding authors: Antonello Baldassarre and Paolo Capotosto

Department of Neuroscience, Imaging and Clinical Sciences, and Institute of Advanced Biomedical Technologies (ITAB), University "G. D'Annunzio" of Chieti-Pescara

Via dei Vestini 33, Chieti Scalo, 66100, Italy

Phone: +39 0871 3556935

E-mail: a.baldassarre@unich.it ; pcapotosto@unich.it

Acknowledgement: This work was supported by the "Departments of Excellence 2018-2022" initiative of the Italian Ministry of Education, University and Research for the Department of Neuroscience, Imaging and Clinical Sciences (DNISC) of the University of Chieti-Pescara. We thank Miriam Curti, Andreana Lavanga and Valentina D'Angelosante for support in training data collection.

Abstract

Individuals are able to improve their visual skill with practice, a phenomenon called Visual Perceptual Learning (VPL). We previously observed that after training on a difficult shape identification task, the dorsal visual regions (i.e. right V2d/V3 and right lateral occipital, LO) corresponding to the trained visual quadrant, and their homologous in the opposite hemisphere, exhibited a selective activation at the end of the learning. By contrast, such modulation was not observed in the ventral visual regions, corresponding to the untrained quadrants. The causal role of the trained visual cortex was previously showed in a TMS study as its inactivation impaired behavioral performance to learned stimuli. Here, using the same experimental design, we employed TMS over the homologous of the trained area (i.e. left V2d/V3) as well as over the untrained region (i.e. right V4) to causally map the visual network during the perceptual learning. We report a decrease of accuracy after TMS over left V2d/V3 as compared to both right V4 and Sham (inactive stimulation) conditions. Importantly, TMS effect was correlated with the degree of learning, such that subjects with lower accuracy at the end of the training exhibited stronger TMS impairment. These results provide evidence that segregated regions within the visual network are causally involved in visual perceptual learning.

Abbreviations: VPL=visual perceptual learning; rTMS= repetitive transcranial magnetic stimulation; LO=lateral occipital; V2d/V3= V2 dorsal V3; pIPS= posterior intraparietal sulcus; FP=false positive.

Introduction

Visual Perceptual Learning (VPL) has been investigated for over a century, and there is solid evidence for changes in neural activity during and after training (Gilbert et al., 2001) (Sasaki et al., 2010) (Shibata et al., 2014). Neurophysiological (Li et al., 2004) and neuroimaging (Yotsumoto et al., 2008) studies have shown changes of neural activity in visual areas induced by training on a visual task. Moreover, several lines of evidence indicated that VPL also induces changes in higher-order level regions involved in the control of visuo-spatial attention and decision-making (Sigman et al., 2005) and changes in the interaction between visual and attention-control systems (Lewis et al., 2009) (Guidotti et al., 2015). In a previous functional MRI study (Lewis et al., 2009) it has been shown that after an intensive training on shape identification task (presented in the left lower visual quadrant), visual and attention-control networks exhibited an opposite pattern of task-evoked activity. Specifically, fronto-parietal regions (i.e. right posterior intraparietal sulcus, pIPS) became less activated for trained as compared to untrained stimuli. By contrast, dorsal visual regions corresponding to the trained (lower left) visual quadrant (i.e. right V2d/V3 and right lateral occipital, LO), exhibited higher activation for familiar shape. Notably, a similar pattern of activity was observed in the homologous of the trained visual cortex (i.e. left V2d/V3), corresponding to the lower right visual quadrant. Conversely, learning-related modulation was not detected in the ventral visual cortices (i.e. right and left V4), corresponding to the untrained upper visual quadrants (Lewis et al., 2009).

Recently, after the intensive training (i.e. the same experimental paradigm of (Lewis et al., 2009), and (Baldassarre et al., 2012)), we employed repetitive transcranial magnetic stimulation (rTMS) in order to investigate the causal role in learning the shape identification task of visual occipital (i.e. right V2d/V3 and LO) and parietal (right pIPS) regions previously shown to be modulated by the training (Baldassarre et al., 2016). We reported that interference with right V2d/V3 and LO, contralateral to the target presentation, affected behavioural responses to learned stimuli as compared to both right pIPS and non-active TMS (Sham) control conditions, thus supporting the causal role of the trained portion of the visual network in the control of the perceptual learning. While the above studies have provided invaluable information on the neural mechanisms of VPL, to date a complete "causal mapping" of the visual network induced by VPL is missing. As a matter of fact, keeping in mind

the above reported data, a more complex pattern of causal involvement within the visual network can be hypothesized, so that, besides main nodes contributing to VPL, also further segregated visual regions might play a causal role. On the light of previous fMRI findings (Lewis et al., 2009), we tested the prediction that, when subjects are trained on a difficult task in the lower left visual quadrant, the impairment in the behavioural performance should be detected also after inactivation of the homologous of the trained visual cortex (i.e. left V2d/V3). On the contrary, no effect should be expected when rTMS is delivered over ventral visual regions (i.e. right V4), which did not show any modulation by VPL. To disclose this open issue, here we directly compared the causal role of different visual regions in the shape identification task performance after an intensive training, delivering rTMS over left V2d/V3, right V4 and vertex (sham), respectively.

Materials and Methods

Subjects and Stimuli

16 right-handed volunteers (age range: 20-30 yrs. old; 5 males) participated in this experiment. A preliminary self-reported questionnaire assessed that they did not present previous psychiatric or neurological history. Participants gave written consent according to the Code of Ethics of the World Medical Association, and the Institutional Review Board and Ethics Committee of the University of Chieti. The experimental protocol was approved by the Institutional Review Board and Ethics Committee of the University of Chieti. The computer monitor was placed in front of them at a distance of about 80 centimeters.

Subjects were trained with daily sessions to attend to the lower left visual quadrant and find the target shape among the distracters while maintaining central fixation. The stimulus array comprised 12 Ts arranged in an annulus of low eccentricity (i.e. 5° radius) and was displayed across the 4 visual quadrants. Of note, with such low eccentricity in our previous study (Lewis et al., 2009) we did not observe significant eye movements. On each trial subjects fixated a central spot for 200 ms (fixation), after which the target shape (an inverted T) was presented at the center of the screen for 2,000 ms (target presentation); finally, an array of 12 stimuli, differently oriented Ts (distracters) with or without an inverted T (target), was briefly flashed for 150 ms (array presentation). The target shape appeared randomly in 1 of 3 locations in the left lower (trained) visual quadrant, and never in the other three untrained quadrants. Subjects attended to the lower left visual quadrant and indicated the presence or absence of the target shape by pressing a left/right mouse button with their right hand (Fig 1a). Overall, subjects are

trained to: (i) attend to the left lower quadrant; (ii) filter unattended information from the distracters in both trained and untrained quadrants; (iii) develop a perceptual template of the target shape. Each block consisted of 45 trials, 36 (80%) that contained the target and 9 (20%) that did not. Training lasted 4-6 days, and an average of 60 practice blocks were necessary to reach a threshold of 80% accuracy in at least 8 consecutive blocks of trials (see Fig. 1b for a representative psychophysical curve). Of note, the accuracy of each block was weighted with the rate of false positive (fp) (Sigman and Gilbert, 2000) (Sigman et al., 2005) (Lewis et al., 2009) (Baldassarre et al., 2016), through the following formula: $p\text{-weighted} = (p - fp) / (1 - fp)$ where p is positive response (i.e. including hits and correct rejection).

When subjects reached criterion, they were asked to perform two blocks of the same task during each TMS condition (i.e. left V2d/V3, right V4, and Sham). Presentation timing was triggered by the TMS train (see below), and the three TMS conditions were run in a counterbalanced order across subjects, who were instructed to respond as accurately and quickly as possible. Reaction times and response accuracy were recorded for behavioral analyses. Notably, none of the subjects reported discomfort or pain during each stimulation site.

Procedures for rTMS and identification of target scalp regions

TMS was delivered through a focal, figure eight coil, connected with a standard Mag-Stim Rapid 2 stimulator (maximum output 2.2 Tesla). Individual resting excitability threshold for right motor cortex stimulation was preliminarily determined following standardized procedure (Rossini et al., 1994). The rTMS train (i.e. 3 pulses) was delivered simultaneously to the central spot ~2 sec before the stimuli array with the following parameters: 150 ms duration, 20-Hz frequency, and intensity set at 100% of the individual motor threshold. The parameters are consistent with published safety guidelines for TMS (Rossi et al., 2009). Of note, previous studies of our group have shown that such inhibition has effect for at least 2 sec, thus affecting target processing (Capotosto et al., 2012a) (Capotosto et al., 2012b) (Capotosto et al., 2015) (Capotosto et al., 2017) (Spadone et al., 2017) (Croce et al., 2018a). All participants performed two active rTMS (i.e. left V2d/V3, right V4) and one inactive TMS (i.e. Sham) conditions corresponding to each stimulation site, applied in different blocks and counterbalanced across subjects. In the "Sham" condition, a pseudo rTMS was delivered at scalp vertex; it was ineffective due to the reversed position of the coil with respect to the scalp surface (i.e. the magnetic flux was dispersed to air). The location of left V2d/V3 and right V4 was automatically identified on

the subject's scalp using the SofTaxic navigator system (E.M.S. Italy, www.emsmedical.net), which permits to compute an estimated volume of head MRIs in subjects for whom MRIs are unavailable. The estimated MRIs are calculated with a warping procedure, by acting on a template MRI volume on the basis of a set of points digitized from the subjects scalp. Specifically, it uses a set of digitized skull landmarks (nasion, inion, and two pre-auricular points), and about 40 scalp points entered with a Fastrak Polhemus digitizer system (Polhemus), and an averaged stereotaxic MRI atlas brain in Talairach space (Talairach and Tournoux, 1988). The average Talairach coordinates in the SofTaxic navigator system were transformed through a linear transformation to each individual subject's scalp. Such method has an error of about 5 mm over a method in which each subject's own MRI is used for localization (Carducci and Brusco, 2012), thus presenting an error lower than the TMS spatial resolution itself (i.e. 1 cm). This individualized head model preserves the anatomical scalp–brain correlates of a mean MR template, providing an accurate set of estimated MRI data, specific for the subject under examination. This approach has been widely and successfully utilized in previous rTMS studies by our and several other groups using a number of subjects comparable with the present study and investigating disparate cognitive domains (Croce et al., 2018a) (Croce et al., 2018b) (Capotosto et al., 2014) (Capotosto et al., 2018) (Sestieri et al., 2013) (Passeri et al., 2015) (Candidi et al., 2011). A mechanical arm maintained the handle of the coil angled at about 45° away from the midline and the centre of the coil wings was positioned on the scalp, to deliver the maximum rTMS intensity over each site (individual peak of activation). The coordinates of the different cortical regions were based on our previous perceptual learning study (Lewis et al., 2009) and were as follows: left V2d/V3 = -10, -85, 01 (x, y, z); right V4 = 23, -75, -12 (x, y, z) (Figure 2a). Importantly, rTMS was delivered ~2 seconds before stimulus array so that the effect was not predominantly on stimulus-evoked activity, which could have been 'masked' by the TMS, but either on preparatory or ongoing activity.

Statistical analyses

Statistical analyses were conducted using within-subject ANOVAs for repeated measures. Mauchley's test was used to evaluate sphericity assumption, Green-house-Geisser procedure was used to correct degrees of freedom, and Duncan tests for post-hoc comparisons ($p < 0.05$).

Firstly, to verify that behavioral deficits induced by rTMS did not reflect a cumulative effect, we computed a t-test comparing the percentage of correct response in the last

day of the training (i.e. last 8 blocks in which subjects reached the criterion) with the accuracy in the Sham condition.

The main statistical design was computed to investigate the causal role of the two visual nodes (i.e. left V2d/V3, right V4) in the perceptual learning task. To this aim we carried out an Anova using percentage of correct responses or reaction times (RTs) with Condition (left V2d/V3, right V4 and Sham) as within-subject factors. Moreover, a similar statistical design tested differences of false positive alarms across TMS conditions.

Finally, to verify whether the behavioral impairment induced by TMS interference was associated with the extent of learning, we carried out several correlation analyses (Pearson test, $p < 0.05$) between accuracy in the last training day (i.e. learning) and the difference of accuracy computed in a pair-wise manner across all experimental conditions (i.e. left V2d/V3, right V4 and Sham). Specifically we used the following differences: left-LO minus right V4, left V2d/V3 minus Sham, right V4 minus Sham.

Results

Several subjects in the last training day performed largely above the criterion (i.e. good learners). As a matter of fact, on average the percentage of correct responses was $89.4 \% \pm 1.2$ SE. Importantly, such score was not significantly different ($p = 0.55$) from the accuracy in the Sham condition ($89.9 \% \pm 1.5$ SE). Since the experimental conditions were counterbalanced across subjects, and the Sham condition may be presented before or after one or two TMS active conditions, the above t-test suggests no cumulative effect of TMS interference.

The results clearly indicated that correct responses occurred less frequently after left V2d/V3 as compared to both Sham and right V4 inhibition (Fig. 2b). This was confirmed by an ANOVA on accuracy that showed a main effect of Condition ($F_{2,30} = 4.45$ $p < 0.02$) with a significant reduction of the percentage of correct responses after left V2d/V3 ($85.6 \% \pm 2.3$ SE) as compared to right V4 ($90.0 \% \pm 1.3$ SE; $p = 0.018$) and Sham ($89.9 \% \pm 1.5$ SE; $p = 0.016$). Importantly, no differences were observed between accuracy after the active (right V4) and inactive (Sham) control conditions ($p = 0.96$). Finally, the same statistical design using RTs did not provide any statistically significant difference across conditions. In Table 1 are reported the RTs for all TMS conditions. Of note, the average of false positive (FP) responses was lower than 20 % across TMS conditions (Table 2). Although TMS over V2d/V3, compared to V4 and Sham conditions, produced slightly higher number of FPs, it

was not statistically different ($p>0.2$), suggesting that TMS impaired the whole behavioral performance.

Interestingly, the percentage of correct responses reached at the end of the training was positively correlated across subjects with the impairment produced by left V2d/V3 inhibition compared to both the active control condition (left V2d/V3 minus right V4) ($r=0.58$; $p=0.018$) (Fig.3a) and the inactive control condition (left V2d/V3 minus Sham) ($r=0.58$; $p=0.019$) (Fig.3b). Conversely, the difference of accuracy between right V4 and Sham was not correlated with the percentage of correct responses at the end of the training ($r=-0.05$; $p=0.83$) (Fig.3c). Overall, these correlations suggest that the magnetic interference was more pronounced in subjects with lower learning degree.

Discussion

In the present study, we used a causal approach to compare the role of two different occipital areas (i.e. left V2d/V3 and right V4), belonging to the visual network involved in Visual Perceptual Learning (VPL). We report that when subjects are trained on the shape identification task in the lower left visual quadrant, the magnetic stimulation of the ipsilateral dorsal visual area (left V2d/V3), but not of the contralateral ventral visual area (right V4), significantly affected the whole behavioural performance. Furthermore, such impairment was stronger in “bad-learner” subjects, as indexed by lower accuracy at the end of the training. These findings provide causal evidence that VPL might be mediated in segregated regions within the visual network.

In the same experimental paradigm, we previously showed that activity in the portion of the trained visual cortex (i.e. right V2d/V3) corresponding to the attended (left) visual quadrant is causally relevant for the processing of learned visual shapes (Baldassarre et al., 2016). By contrast, the interference with higher order parietal region (intra-parietal sulcus, IPS), involved early on the training, did not affect the learning degree. Here, for the first time, a causal role was associated to the homologous of the trained visual cortex (i.e. left V2d/V3) in the control of the perceptual learning. Current result corroborates correlative findings reported in our previous fMRI (Lewis et al., 2009) showing that the homologous of the trained visual cortex exhibited learning specific modulation (higher activation for trained compared to untrained shapes). Conversely, such pattern of causal topography in the visual cortex might not be expected in experimental tasks using central stimuli

displayed at lower eccentricity as suggested by correlative finding by Sigman and colleagues (2005), reporting bilateral quadrant-specific modulation in early visual cortex (V1 and V2). Furthermore, the present results are consistent with evidence indicating that modulations in the visual cortex are not constrained within the attended locations but are extended in the opposite hemisphere homologous to the attended ones (Sylvester et al., 2007) (Tootell et al., 1998). This pattern might reflect attentional mechanisms based on brain activity modulation induced by difference between attended and unattended locations (Sylvester et al., 2007). Notably, in our previous TMS study (Baldassarre et al., 2016) we reported an increase of RT after TMS of the trained visual cortex, whereas here we observed a decrement of accuracy after inhibition of left V2d/V3 (the homologous of the trained visual cortex). Interestingly, a recent model posed that effect on RT is accounted by multiple cognitive processes, whereas effect on accuracy is explained by a single operation (van Ede et al., 2012). Within this framework, it can be speculated that a delay to response after TMS over the trained visual cortex is the consequence of two processes, namely the interference with spatial attention and disruption of the template of the learned shape developed selectively in the trained visual cortex. On the contrary, decreased accuracy after untrained visual cortex inhibition might reflect a single attentional process. Since TMS was delivered nearly 2 second prior to stimulus presentation, hence interfering with preparatory and/or ongoing activity, the more likely possibility is that magnetic stimulation interferes with attentional processes.

Another plausible explanation of the involvement of the ipsilateral visual area (i.e. left V2d/V3) in the processing of the learned shape in the left-lower quadrant may be due to the robust functional connectivity between two homologous regions belonging to the visual network (Lu et al., 2017). This latter interpretation is also strengthened by the observation that both trained visual cortex and its homologous exhibit a similar pattern of learning-induced modulation of functional connectivity as both regions became more negatively correlated with fronto-parietal dorsal attention network after training (Lewis et al., 2009).

A second observation of the present report is that the magnetic stimulation over the learning irrelevant portion of the visual network (i.e. V4) did not affect behavioral performance. This result is in line with the referenced fMRI study (Lewis et al., 2009) showing that learning related modulation was not detected in the ventral visual cortices (i.e. right and left V4). Our finding might reflect the process of filtering out distracters displayed in the "untrained" quadrant (upper-left) represented in the

right ventral visual region (V4). Such operation is less required as the task is learned, hence, unaffected by the stimulation at the end of the training. This explanation may be in line with observation that VPL induced reduction of anticorrelation between right V4 and regions belonging to the so-called Default-mode network which are involved in filtering attended information (Shulman et al., 2003).

Another interesting finding of the current study is that the impairment produced by left V2d/V3 inhibition compared to the active and inactive control conditions is positively correlated with the percentage of correct responses reached at the end of the training. In a previous fMRI study (Baldassarre et al., 2012) we showed that the strength of pre-training resting state functional connectivity between stimulus-related visual regions was positively correlated with a measure of subsequent learning. Specifically, observers with better degree of learning exhibited higher FC, whereas bad learners showed lower extent of synchronization within the visual network. In this framework, it can be speculated that a weaker behavioral effect on good learners after inactivation of a key visual region (left V2d/V3) might be due to their more robust set of functional connections within the visual network. By contrast, bad learners would exhibit a more "vulnerable" visual network as indexed by lower FC, therefore, the interference over a crucial visual node would produce a more pronounced impairment.

Taken together, current and previous findings of our group indicate a topographical causal organization of the visual network during VPL, which was previously observed only using a correlative (fMRI) approach, thus broadening neuroscientific knowledge of this crucial ability as well as of visual cortex functions. From a clinical point of view, these results may provide insights for the therapeutic intervention and recovery in brain disorders involving visual system. Indeed, several previous studies showed that visual perceptual learning can be used as a tool for the treatment of amblyopia, which is a disorder characterized by a reduction of visual acuity in absence of apparent ocular disease (see (Levi and Li, 2009) for a Review). Another pathology of visual system treated through VPL is the macular degeneration (MD), which is the leading cause of blindness in the elderly population. Interestingly, a recent study on MD patients showed a learning induced improvement suggesting a partial cortical reorganization (Maniglia et al., 2018). The present causal topography of the visual system may contribute to better understand the neural mechanisms underlying the recovery of visual functions in these clinical populations. Moreover, our results might pave the way for further studies of 'causal mapping' of brain regions involved in other forms of learning e.g., motor.

References

- Baldassarre, A., Capotosto, P., Committeri, G., Corbetta, M., 2016. Magnetic stimulation of visual cortex impairs perceptual learning. *Neuroimage* 143, 250-255.
- Baldassarre, A., Lewis, C.M., Committeri, G., Snyder, A.Z., Romani, G.L., Corbetta, M., 2012. Individual variability in functional connectivity predicts performance of a perceptual task. *Proc Natl Acad Sci U S A* 109, 3516-3521.
- Candidi, M., Stienen, B.M., Aglioti, S.M., de Gelder, B., 2011. Event-related repetitive transcranial magnetic stimulation of posterior superior temporal sulcus improves the detection of threatening postural changes in human bodies. *J Neurosci* 31, 17547-17554.
- Capotosto, P., Babiloni, C., Romani, G.L., Corbetta, M., 2012a. Differential contribution of right and left parietal cortex to the control of spatial attention: a simultaneous EEG-rTMS study. *Cereb Cortex* 22, 446-454.
- Capotosto, P., Babiloni, C., Romani, G.L., Corbetta, M., 2014. Resting-state modulation of alpha rhythms by interference with angular gyrus activity. *J Cogn Neurosci* 26, 107-119.
- Capotosto, P., Baldassarre, A., Sestieri, C., Spadone, S., Romani, G.L., Corbetta, M., 2017. Task and Regions Specific Top-Down Modulation of Alpha Rhythms in Parietal Cortex. *Cereb Cortex*.
- Capotosto, P., Corbetta, M., Romani, G.L., Babiloni, C., 2012b. Electrophysiological correlates of stimulus-driven reorienting deficits after interference with right parietal cortex during a spatial attention task: A TMS-EEG study. *J Cogn Neurosci* 24, 2363-2371. .
- Capotosto, P., Della Penna, S., Pizzella, V., Zappasodi, F., Romani, G.L., Ilmoniemi, R.J., Brancucci, A., 2018. Theta-burst stimulation causally affects side perception in the Deutsch's octave illusion. *Sci Rep* 8, 12844.
- Capotosto, P., Spadone, S., Tosoni, A., Sestieri, C., Romani, G.L., Della Penna, S., Corbetta, M., 2015. Dynamics of EEG rhythms support distinct visual selection mechanisms in parietal cortex: a simultaneous transcranial magnetic stimulation and EEG study. *J Neurosci* 35, 721-730.
- Carducci, F., Brusco, R., 2012. Accuracy of an individualized MR-based head model for navigated brain stimulation. *Psychiatry Res* 203, 105-108.
- Croce, P., Zappasodi, F., Capotosto, P., 2018a. Offline stimulation of human parietal cortex differently affects resting EEG microstates. *Sci Rep* 8, 1287.
- Croce, P., Zappasodi, F., Spadone, S., Capotosto, P., 2018b. Magnetic stimulation selectively affects pre-stimulus EEG microstates. *Neuroimage* 176, 239-245.
- Gilbert, C.D., Sigman, M., Crist, R.E., 2001. The neural basis of perceptual learning. *Neuron* 31, 681-697.
- Guidotti, R., Del Gratta, C., Baldassarre, A., Romani, G.L., Corbetta, M., 2015. Visual Learning Induces Changes in Resting-State fMRI Multivariate Pattern of Information. *J Neurosci* 35, 9786-9798.
- Levi, D.M., Li, R.W., 2009. Perceptual learning as a potential treatment for amblyopia: a mini-review. *Vision Res* 49, 2535-2549.
- Lewis, C.M., Baldassarre, A., Committeri, G., Romani, G.L., Corbetta, M., 2009. Learning sculpts the spontaneous activity of the resting human brain. *Proc Natl Acad Sci U S A* 106, 17558-17563.
- Li, W., Piech, V., Gilbert, C.D., 2004. Perceptual learning and top-down influences in primary visual cortex. *Nat Neurosci* 7, 651-657.
- Lu, K.H., Jeong, J.Y., Wen, H., Liu, Z., 2017. Spontaneous activity in the visual cortex is organized by visual streams. *Hum Brain Mapp* 38, 4613-4630.
- Maniglia, M., Soler, V., Cottureau, B., Trotter, Y., 2018. Spontaneous and training-induced cortical plasticity in MD patients: Hints from lateral masking. *Sci Rep* 8, 90.
- Passeri, A., Capotosto, P., Di Matteo, R., 2015. The right hemisphere contribution to semantic categorization: a TMS study. *Cortex* 64, 318-326.
- Rossi, S., Hallett, M., Rossini, P.M., Pascual-Leone, A., 2009. Safety, ethical considerations, and application guidelines for the use of transcranial magnetic stimulation in clinical practice and research. *Clin Neurophysiol* 120, 2008-2039.

- Rossini, P.M., Barker, A.T., Berardelli, A., Caramia, M.D., Caruso, G., Cracco, R.Q., Dimitrijevic, M.R., Hallett, M., Katayama, Y., Lucking, C.H., et al., 1994. Non-invasive electrical and magnetic stimulation of the brain, spinal cord and roots: basic principles and procedures for routine clinical application. Report of an IFCN committee. *Electroencephalogr Clin Neurophysiol* 91, 79-92.
- Sasaki, Y., Nanez, J.E., Watanabe, T., 2010. Advances in visual perceptual learning and plasticity. *Nat Rev Neurosci* 11, 53-60.
- Sestieri, C., Capotosto, P., Tosoni, A., Luca Romani, G., Corbetta, M., 2013. Interference with episodic memory retrieval following transcranial stimulation of the inferior but not the superior parietal lobule. *Neuropsychologia* 51, 900-906.
- Shibata, K., Sagi, D., Watanabe, T., 2014. Two-stage model in perceptual learning: toward a unified theory. *Ann N Y Acad Sci* 1316, 18-28.
- Shulman, G.L., McAvoy, M.P., Cowan, M.C., Astafiev, S.V., Tansy, A.P., d'Avossa, G., Corbetta, M., 2003. Quantitative analysis of attention and detection signals during visual search. *J Neurophysiol* 90, 3384-3397.
- Sigman, M., Gilbert, C.D., 2000. Learning to find a shape. *Nat Neurosci* 3, 264-269.
- Sigman, M., Pan, H., Yang, Y., Stern, E., Silbersweig, D., Gilbert, C.D., 2005. Top-down reorganization of activity in the visual pathway after learning a shape identification task. *Neuron* 46, 823-835.
- Spadone, S., Sestieri, C., Baldassarre, A., Capotosto, P., 2017. Temporal dynamics of TMS interference over preparatory alpha activity during semantic decisions. *Sci Rep* 7, 2372.
- Sylvester, C.M., Shulman, G.L., Jack, A.I., Corbetta, M., 2007. Asymmetry of anticipatory activity in visual cortex predicts the locus of attention and perception. *Journal of Neuroscience*.
- Talairach, J., Tournoux, P., 1988. *Co-Planar Stereotaxic Atlas of the Human Brain*. Thieme Medical Publishers, Inc., New York.
- Tootell, R.B.H., Hadjikhani, N., Hall, E.K., Marrett, S., Vanduffel, W., Vaughan, J.T., Dale, A.M., 1998. The retinotopy of visual spatial attention. *Neuron* 21, 1409-1422.
- Yotsumoto, Y., Watanabe, T., Sasaki, Y., 2008. Different dynamics of performance and brain activation in the time course of perceptual learning. *Neuron* 57, 827-833.

Figure and Table Legends:

Table 1: Reaction times (mean and SE) for all TMS conditions.

Table 2: Percentage of false positive responses (mean and SE) for all TMS conditions.

Figure 1: a) Example of the experimental task. **b)** Example of a single subject's learning curve. The dotted line indicates the learning threshold of 80% accuracy.

Figure 2: a) Inflated view of left (top) and right (bottom) hemispheres, respectively, atlas brain with regions belonging to the visual networks as in previous work of Lewis et al (2009). Regions with coordinates are stimulated with rTMS in this experiment and are as follows: left V2d/V3: -10, -85, 01 (x, y, z); right V4 23, -75, -12 (x, y, z). **b)** Group means (\pm standard error, SE) of the accuracy (%) for the three rTMS Conditions (left V2d/V3, right V4, Sham). Duncan post-hoc tests: one asterisk ($p < 0.02$).

Figure 3: Scatter-plots showing the linear correlations between accuracy in the last training day (i.e. learning) and the difference of accuracy computed comparing left V2d/V3 minus right V4 **(a)**, Left V2d/V3 minus Sham **(b)**, and right V4 minus Sham **(c)**.

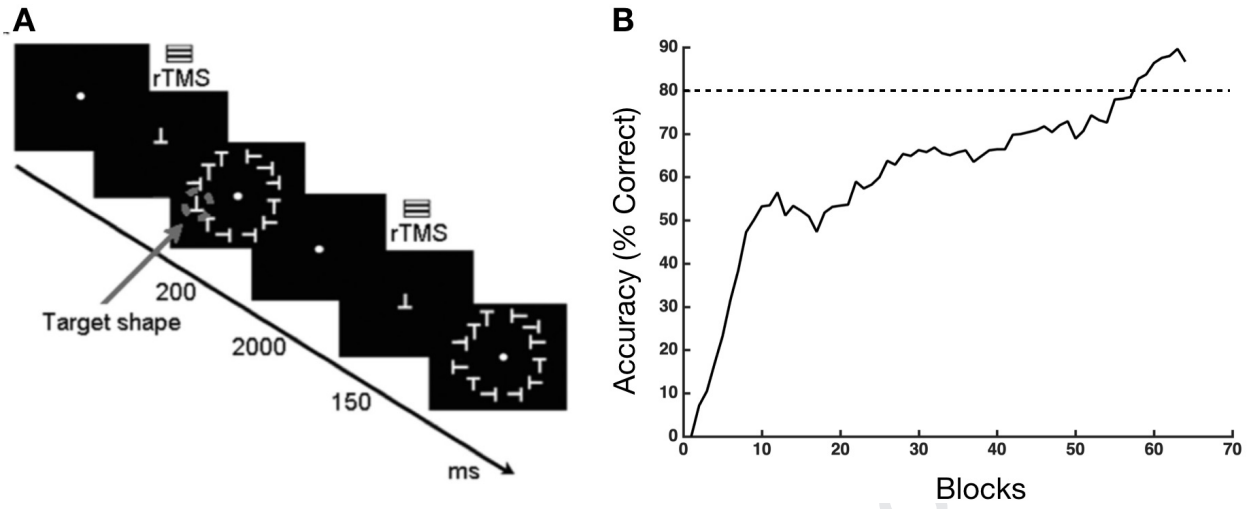
Table 1: RTs for all TMS conditions

	V2dV3	V4	sham
mean	569.5	565.6	558.2
SE	19.4	18.8	17.7

Table 2: FPs for all TMS conditions

	V2dV3	V4	sham
mean (%)	20	14	18
SE (%)	5	3	5

Journal Pre-proof



Journal Pre-proof

